Automatic Detection of Surface Defects on Rolled Steel Using Computer Vision and Artificial Neural Networks

Luiz A. O. Martins, Flávio L. C. Pádua, Paulo E. M. Almeida
Intelligent Systems Laboratory
Federal Center of Technological Education of Minas Gerais
Av. Amazonas, 7675, Belo Horizonte, 30.510-000, MG, Brazil
Email: {luizalberto, cardeal, pema}@lsi.cefetmg.br

***Abstract*—This work addresses the problem of automated visual inspection of surface defects on rolled steel, by using Computer Vision and Artificial Neural Networks. In recent years, the increasing throughput in the steel industry has become the visual inspection a critical production bottleneck. In this scenario, to assure a high rolled steel quality, novel sensor-based technologies have been developed. Unlike most common techniques, which are frequently based on manual estimations that lead to significant time and financial constraints, we present an automatic system based on (i) image analysis techniques, such as, Hough Transform to classify three defects with well-defined geometric shapes: welding, clamp and identification hole and (ii) two well-known feature extraction techniques: Principal Component Analysis and Self-Organizing Maps to classify three defects with complex shapes, specifically, oxidation, exfoliation and waveform defect. To demonstrate the effectiveness of our system, we tested it on challenging real-world datasets, acquired in a rolling mill of the steel company ArcelorMittal. The system was successfully validated, achieving overall accuracy of 87% and demonstrating its high potential to be applied in real scenarios.**

I. Introduction

The outstanding quality requirements and an increased competitive environment has become traditional surface quality control practices (visual inspection) inappropriate for steel makers [1]. The challenge consists in to replace human experts with automatic systems capable of performing constant, round-the-clock surface inspection. The reliability of these systems is critical, since they should guarantee that no critical defect will go undetected, but without generating many false alarms that make the system unusable [2].

Another challenge consists in to perform inspection at locations where it was previously unfeasible due to obstacles, such as, high temperatures. This is for example the case at the hot strip mill, where stakes for early defect detection are enormous: early removal of defective product from the production stream without adding further value; yield reduction due to "traditional" quality control practices (wrap, re-inspection); faster feed-back to upstream plants [3], [4].

As an effort to face those challenges, vision-based automatic systems have been frequently proposed. These systems have matured considerably over the last years, due to advances in enabling technologies like sensors, processor hardware, software methodologies, and networking to list just a few [5]. These advances in cost, performance and design methodologies have resulted in an explosion of application areas [6].

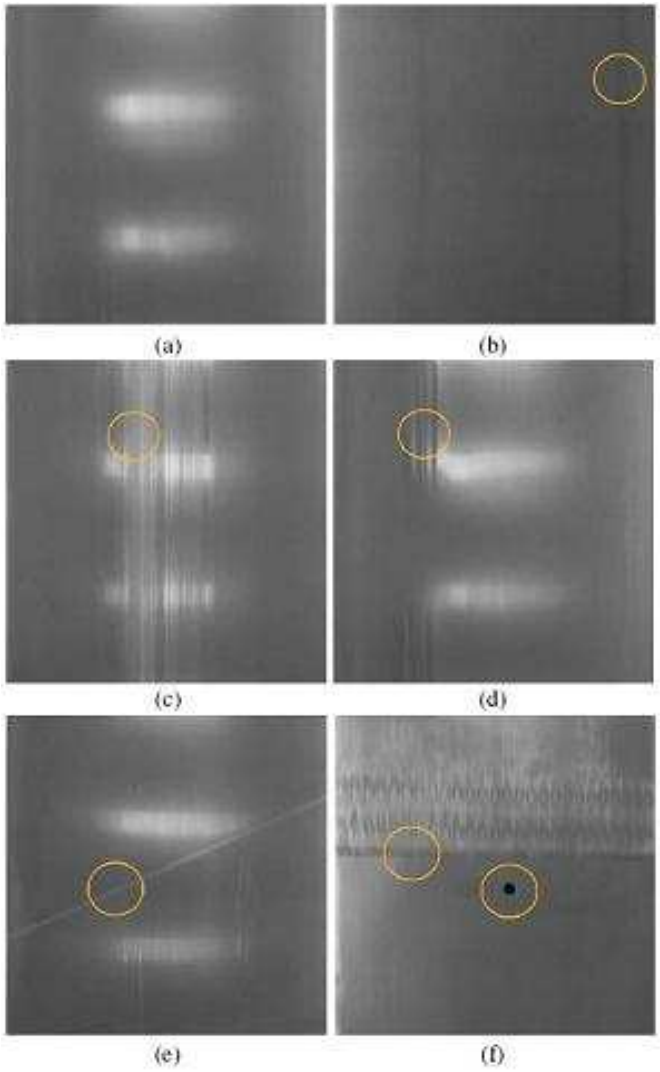

Fig. 1. Image samples containing the six surface defects considered. (a) Sample without defects, (b) Oxidation, (c) Exfoliation, (d) Waveform defect, (e) Welding and (f) Clamp and identification hole.

978-1-4244-5226-2/10/$26.00 ©2010 IEEE

According to Jia et al. [1], a reliable vision-based system for detecting surface defects on rolled steel automatically should be able to handle cases like: *bad image quality*, *online usage*, *defects variability*, *segmentation failures* e *environmental variations*.

As a step toward this goal, we developed a system that operates under all of the above conditions except the last one. Specifically, it considers that images are acquired by a single stationary calibrated camera and assumes that scene illumination is stabilized. The proposed automatic system is based on (i) image analysis techniques, such as, Hough Transform to classify three defects with well-defined geometric shapes: welding, clamp and identification hole and (ii) two well-known feature extraction techniques: Principal Component Analysis and Self-Organizing Maps to classify three defects with complex shapes: oxidation, exfoliation and waveform defect. Image samples containing the six surface defects considered in this work are presented in Fig. 1.

Surveys on several techniques for automated visual inspection of surface defects can be found in [6]–[8]. In [9], the authors present a fuzzy expert system for strip steel surface quality evaluation. The expert system is composed by six parts: knowledge base, rule base, HMI, inference engine, knowledge acquiring mechanism and explanation mechanism. The core of the expert system is the design of knowledge explanation, rule base and inference engine, being capable to rank and price the steel coil products according to the surface quality.

In [10], the authors propose a real-time defect detection method for high-speed steel bar in coil. A detection algorithm based on laplacian operation, an edge-preserving filter and a double thresholding method are used. The system operates in real-time and a detection rate of 95.42% was reported. In [11], the authors present a method that detects surface defects with three-dimensional characteristics on scale-covered steel blocks. Depth maps are computed and segments of the surface are classified according to a set of extracted features by means of Bayesian network classifiers. The structure of the Bayesian network is determined by a floating search algorithm. A classification rate of 98% was reported in this work.

Jia et al. [1] describe a real-time visual inspection system that uses support vector machines to automatically detect steel surface defects (seams) in a hot mill process. An overall accuracy of 94.4% was achieved. Similarly to that approach, the authors in [2] use support vector machines and principal component analysis to detect and classify fabric defects, such as, *double-weft*, *netting-multiplies* and *slack-pick*, in several industrial textured materials.

In [12], an inspection system has been developed to detect structural defects on bumpy metallic surfaces, specially, holes and cracks on the surfaces of aluminium. The system is based on morphology and genetic algorithms and was validated with a database collected from industrially produced aluminium samples, achieving overall accuracy as high as 91%.

Lee et al. [13] have used neural networks to classify defects in cold rolled steel strips through energy and entropy features computed from the adaptive wavelet packet expansion of the steel images. The defects considered in this work were: contamination, the dull mark, the rust, the scab, the scratch, the black line, the heat buckle and the hole. For the test sets considered, 99% of defects were classified correctly.

Finally, in [4], an automated visual metal strip inspection system is described. The system is capable of classifying surface defects in copper alloy strips and it was installed for evaluation in a mill production line. The proposed algorithms are based on morphological preprocessing and combined statistical and structural defect recognition.

The remainder of this paper is organized as follows: Sections 2 covers our automatic system for detection of surface defects. Experimental results are presented in Section 3, followed by the conclusions and discussion in Section 4.

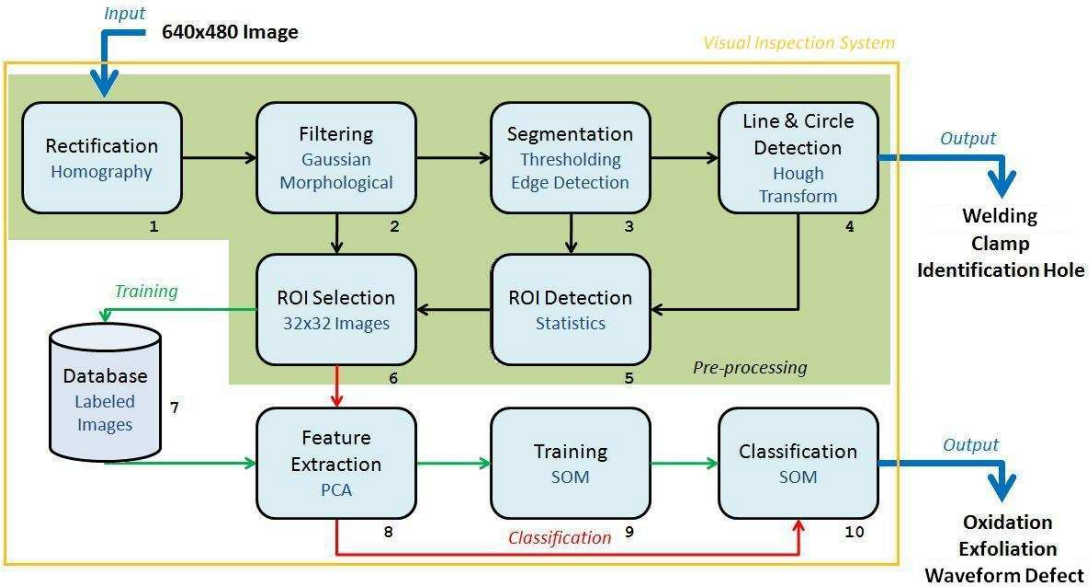

Fig. 2. Block diagram of the proposed system for visual inspection of surface defects on rolled steel plates.

II. Visual Inspection System

The operation of the proposed system can be divided in three modules: input, inspection and output as shown in Fig. 2. The input module refers basically to images acquisition and delivering of them to the inspection one using Computer Vision techniques and Artificial Neural Networks. It sends to the output module these images rectified, with defects detected and classified per region.

The operation of the inspection module is performed in three steps: pre-processing, training and classification. Firstly, image rectification (block 1) is performed, which aims to eliminate lens distortions and to transform the image perspective so that the defect position on the rolled steel can be identified accurately. Camera calibration techniques are used.

After rectification, the next operation consists of eliminating noises caused by lighting variation or other unwanted noise source during the images acquisition. This operation (block 2) is carried out by applying Gaussian and morphological filters on the image rectified. It results in a gray scale image of the rolled steel surface detaching the gray level variations.

After filtering, the image is submitted to the operation of segmentation (block 3). Segmentation is realized by applying a thresholding on the image filtered that result in a binary image. Throughout this binary image is possible to distinguish the table of inspection to the rolled steel. So, using an edge detection method, the steel position on the table is identified and an automatic width measurement system can be defined.

The binary image is also submitted to lines and circles detection (block 4). This operation is basically performed using Hough Transform as shown in Fig. 3. Using this technique, three types of defects can be classified: welding, characterized by a diagonal line in relation of the strip edge; clamp, characterized by a perpendicular line at the same condition; and identification hole, characterized by a circle with fixed radius in the middle of the strip.

The operation of detecting the region of interest (block 5) consists on applying a grid over the image binarized (block 3). Each region of this grid is defined as sub-image of 32x32 pixels. Grid positions with a quantity of non null pixels over a limit and without any line or cycle are processed by the next operation (block 6).

The operation of selecting interest region (block 6) receives localizations of grid regions (block 5) to be tested and to select in the image filtered (block 2) the 32x32 sub-images that will be used by the system. This operation finishes the pre-processing phase. So, the final result is the delivering of sub-images to training and classification steps.

During the training step, the sub-images are stored in a database (block 7) where they are identified and selected according to their classes: waveform defect, exfoliation or oxidation.

Since the database has been constituted, the training step starts with the operation of feature extraction (block 8) using the Principle Component Analysis (PCA) technique. This operation performs an important issue by representing and keeping main details of each defect.

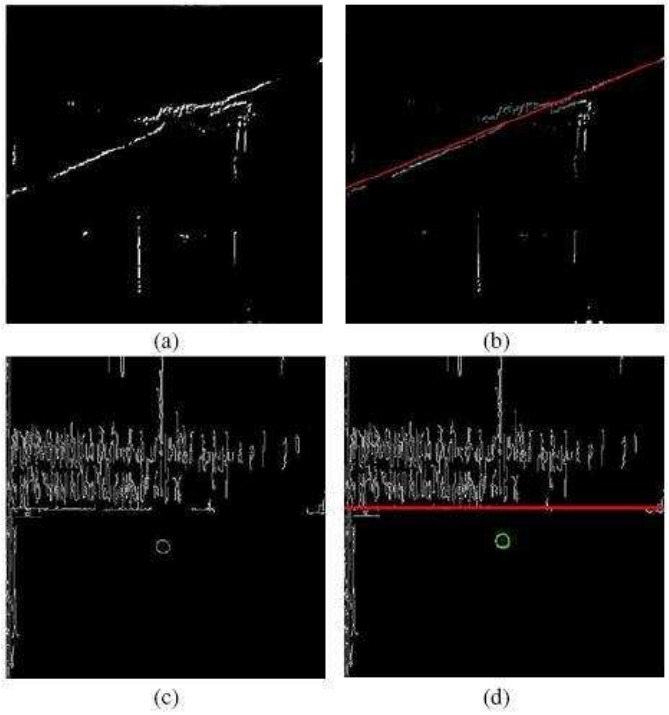

Fig. 3. Line and circle detection by using Hough Transform to classify: (a)-(b) Welding and (c-)(d) clamp with identification hole.

After feature extraction, samples are used to train a Self-Organizing Map (SOM) classifier (block 9).

Once the training has been done, the regions defined in the pre-processing step (block 6) are classified. The classification step runs on line and performs features extraction (block 8) and classification (block 10) operations. Regions candidates are submitted directly to the extractor and classifier. The output module presents the results.

A. Hough Transform Based Line and Circle Detection

The basic theory of the Hough line transform is that any point in a binary image could be part of some set of possible lines. If we parameterize each line by a slope a and an intercept b from the equation $y = ax + b$, then a point in the original image is transformed to a locus of points in the (a, b) plane corresponding to all of the lines passing through that point. After converting every nonzero pixel in the input image into such a set of points in the output image and sum over all such contributions, then lines that appear in the input image, (x, y) plane, will appear as local maxima in the output image, (a, b) plane, called as accumulator plane. To avoid the problem that vertical lines give rises to unbounded values of the parameters *a* and *b*, the preferred parametrization represents each line as a point in polar coordinates (ρ, θ), from the equation $\rho = xcos\theta + y$. The Hough circle transform works in a manner analogous to the Hough line transforms. In this case, the accumulator plane is replaced by an accumulator volume with three dimensions: one for *x*, one for *y*, and another for the circle radius *r*.

B. PCA-Based Feature Extraction

PCA is a standard technique for dimensionality reduction and has been applied to a broad class of problems. Although PCA presents some shortcomings, such as its implicit assumption of Gaussian distributions and its restriction to orthogonal linear combinations, it remains popular due to its simplicity. The idea of applying PCA to object classification is not novel [14], [15]. Our contribution lies in rigorously demonstrating that PCA is well-suited to parameterize three defects with complex shapes: oxidation, exfoliation and waveform defect.

Given p grayscale image samples, we obtain for each sample i ($i = 1, 2, \ldots, p$) one n-dimensional column vector $\mathbf{v}_i$, by concatenating the n pixel values. Those n-dimensional column vectors are combined to form a matrix Υ, as follows:

$$\Upsilon = [\mathbf{v}_1 \quad \mathbf{v}_2 \quad \ldots \quad \mathbf{v}_p], \tag{1}$$

In the following, we describe the application of PCA to Υ.

Consider a new coordinate system $T = [\mathbf{t}_1 \quad \mathbf{t}_2 \quad \ldots \quad \mathbf{t}_p]$. Supposing that T is orthonormal, the representation $\hat{\Upsilon}$ of Υ in this new system is given by:

$$\hat{\Upsilon} = T^\top \Upsilon. \tag{2}$$

Assuming that $\mathbf{v}_i$ has expected value zero, that is, $E[\mathbf{v}_i] = \mathbf{0}, \forall i$, we compute the covariance matrix of $\hat{\Upsilon}$ as follows:

$$\sigma^2 = T^\top R T, \tag{3}$$

where $R = E\left[\Upsilon\Upsilon^\top\right] \simeq \frac{1}{p}\Upsilon\Upsilon^\top$.

The coordinate system T that results in the highest possible value for covariance is computed by finding a singular value decomposition for R, as follows:

$$R = \Lambda\Sigma\Omega^\top. \tag{4}$$

As R is symmetric, we have $\Lambda = \Omega$, that is, $R = \Omega\Sigma\Omega^\top$. After some additional mathematical manipulations, we get:

$$\Sigma = \Omega^\top R \Omega, \tag{5}$$

where the main diagonal of Σ contains the singular values of $\Omega^\top R\Omega$. Assuming that $T = \Omega$ and comparing Equations (3) and (5), we note that $\sigma^2 = \Sigma$.

Given that matrix R represents the correlation between the coordinates of each vector $\mathbf{v}_i$ of Υ, $\forall i$, the transformation applied to R in Equation 5 performs its diagonalization, representing R in a new orthogonal system. In this new coordinate system given by T, each coordinate j of a vector $\mathbf{v}_i$ presents maximum variance with respect to axis $\mathbf{t}_j$ and null variance with respect to the other axes. It is exactly this property that allows the dimensionality reduction of data.

Therefore, by using only the first k vectors of T, that is, $T_k = [\mathbf{t}_1 \quad \mathbf{t}_2 \quad \ldots \quad \mathbf{t}_k]$, the representation of Υ in this new coordinate system is given by:

$$\hat{\Upsilon}_k = T_k^\top \Upsilon. \tag{6}$$

C. SOM-Based Defect Classification

A self-organizing map (SOM) is a type of artificial neural network that is trained using unsupervised learning to produce a low-dimensional representation of the input space of the training samples, called a map. Self-organizing maps are different from other artificial neural networks in the sense that they use a neighborhood function to preserve the topological properties of the input space.

Neurons of a SOM network are organized in a grid, commonly bi-dimensional. In this bi-dimensional grid, output neurons are organized in rows and columns. Neurons are connected to the adjacent ones by a neighborhood relation, describing the topology or structure of the map. The SOM topology shapes can be rectangular or hexagonal. The best shape depends on the problem considered and the distribution of data.

The SOM is trained iteratively. In each training step, one sample $\mathbf{v}$ from the input dataset is chosen randomly and a similarity measure is calculated between it and all the weight vectors of the map. The Best-Matching Unit (BMU), denoted as *c*, is the unit whose weight vector has the greatest similarity with the input sample $\mathbf{v}$. The similarity is usually defined by means of a distance measure, typically Euclidian distance. Formally the BMU is defined as the neuron for which:

$$\| \mathbf{v} - \mathbf{w}_c \| = \min_i \{\| \mathbf{v} - \mathbf{w}_i \|\}, \tag{7}$$

where $\| \cdot \|$ is the distance measure.

The distance computation used here doesn't consider missing values (eg. it is assumed that their contribution to the distance $\| \mathbf{v} - \mathbf{w}_i \|$ is zero) and apply a mask (weighting factor) for excluding certain variables from the BMU-finding process. With these changes, the distance measure becomes:

$$\| \mathbf{v} - \mathbf{w}_c \|^2 = \sum_{k \epsilon K} m_k (v_k - w_k)^2, \tag{8}$$

where K is the set of known (not missing) variables of sample vector $\mathbf{v}$, v_k and w_k are the k-th components of the sample and weight vectors and m_k is the k-th mask value.

After finding the BMU, the weight vectors of the SOM are updated so that the BMU is moved closer to the input vector in the input space. The topological neighbors of the BMU are treated similarly. This adaption procedure stretches the BMU and its topological neighbors towards the sample vector. The algorithm based on BMU neighborhood concept is commonly called as Winner-Takes-All, since the neuron BMU receives the highest weight updating.

The SOM update rule for the weight vector of unit *i* is:

$$\mathbf{w}_i(t+1) = \mathbf{w}_i(t) + \alpha(t) h_{ci}(t) [\mathbf{v}(t) - \mathbf{w}_i(t)], \tag{9}$$

where $\mathbf{v}(t)$ is an input vector randomly drawn from the input dataset at time *t*, $h_{ci}(t)$ the neighborhood kernel around the winner unit c and $\alpha(t)$ the learning rate at time t. The neighborhood kernel is a non-increasing function of time and of the distance of unit i to the winner unit c. It defines the influence region that the input sample has on SOM network.

III. Experimental Results

To demonstrate the effectiveness of our system, we tested it on a real scenario, by acquiring images in a cold mill line of the steel company ArcelorMittal.

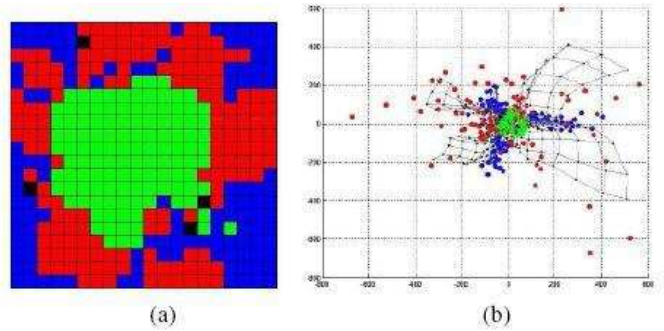

Fig. 4. a) Output map of 20x20 with neurons labeled in red (waveform defect), green (oxidation) and blue (exfoliation). (b) Tridimensional representation of input (samples) in a PCA space and the 20x20 map.

A. Defects with Simple Geometric Shapes

Hough Transform was used to detect lines and circles and, consequently, welding, clamp and identification hole defects. In this case, 300 images of 640x480 pixels were divided in six groups of 50 images for representing each class. The grid region (416x416 pixels) of each image was extracted to complete a data set of 300 samples for testing.

Welding and clamp defects are characterized by the diagonal or horizontal lines, respectively, along the image. So, the line angle was considered to their distinction:

- Welding: $20° \leq \theta \leq 40°$;
- Clamp: $-5° \leq \theta \leq 5°$.

Identification hole is characterized by a circle with fixed radius in the middle of the strip. So, a region of searching was defined to find this circle. Table I shows the results in terms of accuracy to welding, clamp and identification hole defects based on lines and circles detection.

B. Defects with Complex Geometric Shapes

Using sub-images of 32x32 pixels, a database was populated with 5400 samples extracted from gray level images of 640x480 pixels. These samples were distributed according to their classes: exfoliation, oxidation and waveform defect.

All matrixes representing the patterns were submitted to features extraction using the PCA technique. So, it resulted in new matrixes containing representative features of samples.

The major six main components extracted by PCA technique were considered to compose the matrixes of features.

Those matrixes were joined to one PCA matrix with 5400 samples. After randomizing this PCA matrix, eight combinations were taken to the experiments. Two thirds of the samples (3600) were used to train the SOM network while one third (1800) were used to test it. The input samples of each combination were labeled before the SOM network training to determine classes of the output neurons.

Training samples and their respective labels were encapsulated in a structure and an output map of 20x20 rectangular shape was defined. So, the SOM was initialized.

The algorithm of the SOM network try to initialize the map linearly with the two greatest eigenvectors and, in case of calculation failure, it initializes randomly. After initializing, the SOM is trained in two phases: firstly a rough training and so a fine one.

After the training, the output neurons were labeled by the majority vote of samples that they had grouped. In case of equality, the labeling was done according to the nearest neuron. Fig. 4(a) shows the map with squares in blue, green and red meaning respectively exfoliation, oxidation and waveform defects. Squares in black identify non-winner neurons. Figure 4(b) shows some samples in a tridimensional PCA space, using the same colors and the output neurons in black. After training and labeling output neurons, the network performance was measured. Testing samples were labeled also. It was submitted to the network and classified according to the output neuron that has grouped it (winner neuron). The comparison between sample and winner neuron labels determined the network classification accuracy.

Table II shows the results in terms of network classification accuracy. Column "Combination" shows the PCA matrix combinations used and columns "Exfoliation", "Oxidation" and "Waveform Defect" show the results of accuracy for each defect class. Finally, column "Global" shows the results of accuracy considering all defects simultaneously. After carrying out all steps, then the output module presents the images of the Visual Inspection System as showed on Fig. 5.

IV. Conclusion

This work presented a Visual Inspection System to detect and classify rolled steel defects using Computer Vision techniques and Artificial Neural Network. Welding, clamp and identification hole were classified using Hough Transform. Experiments carried out with these defects used 300 samples for testing and gathered classification accuracy results around 98% as showed on Table I.

High accuracy values are justified by the well defined geometric features of each defect (rarely a diagonal line will be find in a clamp image).

The oxidation, exfoliation and wave-mark defects were classified using the typical steps of a pattern recognition system. PCA is a robust technique and used largely to dimensionality reduction or features extraction. Thats why it was used here. The self-organizing characteristic of SOM network makes it so appropriate for grouping classes. This characteristic was explored to get a flexible classifier in terms of group components definition and classes labeling. These two techniques

TABLE I
Classification Accuracy Using Hough Transform

Type of Defect	**Diagonal Lines** (%)	**Horizontal Lines** (%)	**Circles** (%)
Welding	96.00	100.00	100.00
Clamp	100.00	86.36	98.00
Identification Hole	100.00	100.00	100.00
Oxidation	100.00	100.00	100.00
Waveform	100.00	100.00	100.00
Exfoliation	100.00	100.00	94.00
Average	99.33	97.73	98.67

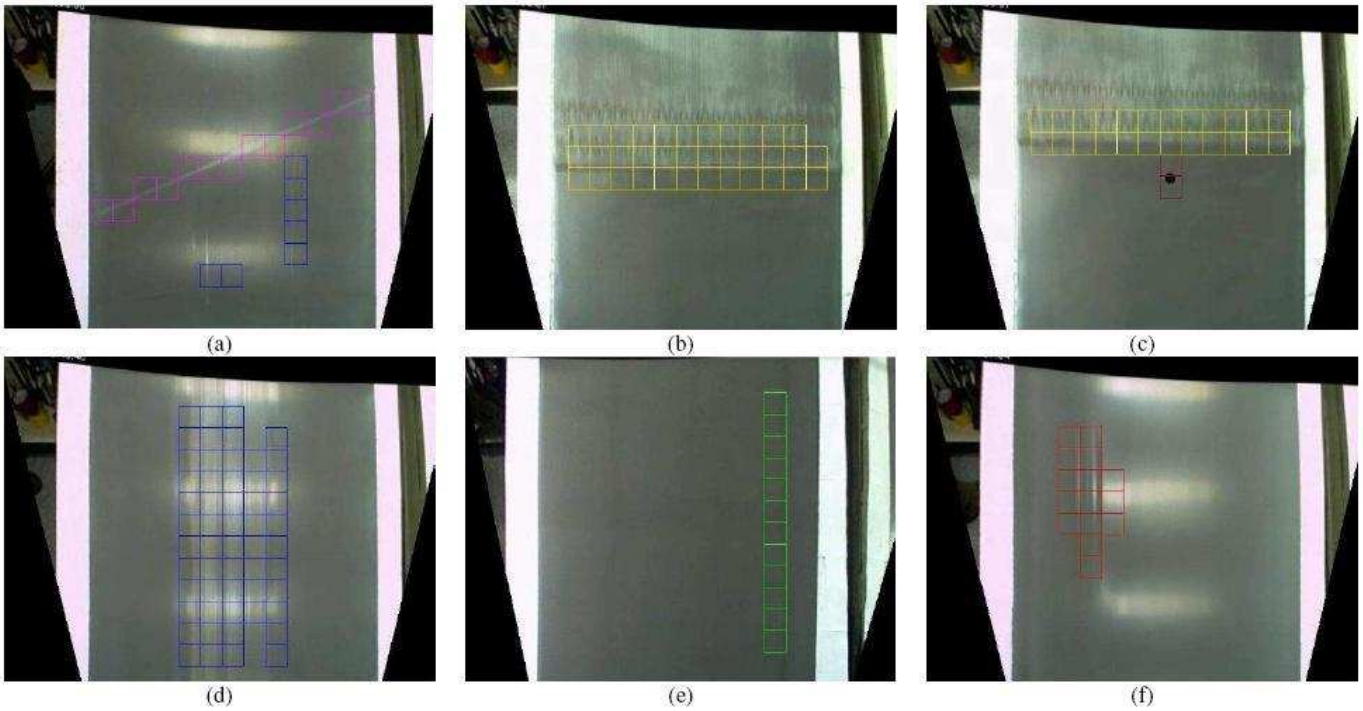

Fig. 5. Images rectified and regions classified according to the defect classes: (a) welding in pink, (b) clamp in yellow, (c) clamp with identification hole in brown, (d) exfoliation in blue, (e) oxidation in green and (f) waveform defect in red.

were combined to develop a potential system that can be used in a real scenario of mill line. The classification system using PCA and SOM achieved an overall classification rate of 77%. Considering the results for the six defects discussed, the overall classification accuracy achieved is 87%.

ACKNOWLEDGMENT

The authors thank FAPEMIG (Proc. PEE-00915-10), CNPq, CAPES and CEFET-MG for the financial support and Arcelor-Mittal for providing the datasets to perform this work.

REFERENCES

[1] H. Jia, Y. Murphey, S. Jinajun, and C. Tzyy-Shuh, "An Intelligent Real-Time Vision System for Surface Defect Detection," in *IEEE International Conference on Pattern Recognition*, 2004, pp. 239–242.

[2] A.Kumar and H. C. Shen, "Texture Inspection for Defects Using Neural Networks and Support Vector Machines," in *IEEE International Conference on Image Processing*, 2002, pp. 353–356.

TABLE II
CLASSIFICATION ACCURACY USING PCA AND SOM

Combination	**Exfoliation** (%)	**Oxidation** (%)	**Waveform Defect** (%)	**Global** (%)
A_1	50.62	98.33	78.55	75.06
A_2	45.38	96.00	79.09	72.56
A_3	50.92	95.50	81.64	75.17
A_4	52.77	95.67	80.55	75.56
A_5	62.00	98.00	78.00	78.89
A_6	68.00	97.50	76.55	80.44
A_7	67.85	94.33	78.18	79.83
A_8	67.69	97.33	74.55	79.67
Average	58.15	96.58	78.39	77.15

[3] Z. Xuezeng, W. Ke, Q. Xifu, and G. Guangxue, "On-Line Inspection Techniques of Manufacturing Quality of Rolled-Steel Sheet," *Jornal of Forestry Research*, vol. 5, no. 3, pp. 41–43, 1994.

[4] T. Piironen, O. Silven, M. PietikŁinen, T. Laitinen, and E. Strmmer, "Automated Visual Inspection of Rolled Metal Surfaces," *Machine Vision and Applications*, vol. 3, no. 4, pp. 247–254, 1990.

[5] M. Shirvaikar, "Trends in Automated Visual Inspection," *Jornal of Real-Time Image Processing*, vol. 1, no. 1, pp. 69–74, 2006.

[6] T. R. Chin and C. A. Harlow, "Automated Visual Inspection: A Survey," *IEEE Transactions on Pattern Analysis and Machine Intelligence*, vol. 4, no. 6, pp. 557–573, 1982.

[7] X. Xie, "A Review of Recent Advances in Surface Defect Detection using Texture analysis Techniques," *Electronic Letters on Computer Vision and Image Analysis*, vol. 7, no. 3, pp. 1–22, 2008.

[8] T. S. Newman and A. K. Jain, "A Survey of Automated Visual Inspection," *Computer Vision and Image Understanding*, vol. 61, no. 2, pp. 231–262, 1995.

[9] Z. Jiuliang, L. Weiwei, Y. Feng, L. Jun, Z. Yao, and Y. Yunhui, "Research on Surface Quality Evaluation System of Steel Strip Based on Computer Vision," in *International Symposium on Intelligent Information Technology Application*, 2009.

[10] J. P. Yun, S. Choi, B. Seo, and S. W. Kim, "Real-Time Vision-Based Defect Inspection for High-Speed Steel Products," *Optical Engineering*, vol. 47, no. 7, p. 077204, 2008.

[11] F. Pernkopf, "Detection of Surface Defects on Raw Steel Blocks Using Bayesian Network Classifiers," *Pattern Analysis and Applications*, vol. 7, no. 1, pp. 333–342, 2004.

[12] H. Zheng, L. X. Kong, and S. Nahavandi, "Automatic Inspection of Metallic Surface Defects Using Genetic Algorithms ," *Journal of Materials Processing Technology*, vol. 125, no. 126, pp. 427–433, 2002.

[13] C. Lee, C. Choi, J. Choi, Y. Kim, and S. Choi, "Feature Extraction Algorithm Based on Adaptive Wavelet Packet for Surface Defect Classification," in *IEEE International Conference on Image Processing*, 1996, pp. 673–675.

[14] M. T. A. Rodrigues, F. L. C. Pádua, and R. M. Gomes, "Automatic Fish Species Classification Based on Robust Feature Extraction Techniques and Artificial Immune Systems," in *IEEE International Conference on Bio-Inspired Computing: Theories and Applications*, 2010.

[15] Y. Ke and R. Sukthankar, "PCA-SIFT: A More Distinctive Representation for Local Image Descriptors," in *IEEE Conference on Computer Vision and Pattern Recognition*, 2004, pp. 506–513.